Cancer Chemother Pharmacol (2011) 68:1585–1594
DOI 10.1007/s00280-011-1608-x

ORIGINAL ARTICLE

Preclinical evaluation of the novel multi-targeted agent R1530

Kenneth Kolinsky · Christian Tovar · Yu-E Zhang · Aruna Railkar · Hong Yang · Daisy Carvajal · Thomas Nevins · Wanping Geng · Michael Linn · Kathryn Packman · Jin-Jun Liu · Zhuming Zhang · Peter Wovkulich · Grace Ju · Brian Higgins

Received: 16 September 2010 / Accepted: 3 March 2011 / Published online: 8 May 2011

Abstract
Purpose This study describes the antiproliferative activity of the multikinase inhibitor R1530 in vitro and its antitumor and anti-angiogenic activity, pharmacokinetics, and tolerability in vivo.
Methods The antiproliferative activity of R1530 was investigated in a range of human tumor, endothelial and fibroblast cell lines. Tolerability and antitumor activity were assessed in mice bearing a range of human tumor xenografts, and anti-angiogenic properties were established in the murine corneal pocket assay. R1530 pharmacokinetics in mice were established.
Results R1530 strongly inhibited human tumor cell proliferation. Growth factor-driven proliferation of endothelial and fibroblast cells was also inhibited. Significant tumor growth inhibition was demonstrated in a lung cancer xenograft model with a range of once daily, weekly and twice-weekly doses of R1530 (3.125–50 mg/kg qd, 100 mg/kg qw, 100 mg/kg biw). Daily doses were most effective in the lung cancer model and also had significant growth inhibitory effects in models of colorectal, prostate, and breast tumors. Tumor regression occurred in all models treated with the maximum tolerated daily dose (50 mg/kg). The doses of 25 and 50 mg/kg qd resulted in biologically significant increased survival in all tested models. After oral administration in nude mice, R1530 showed good tissue penetration. Exposure was dose dependent up to 100 mg/kg with oral administration.
Conclusions R1530 has demonstrated activity against a range of tumor models in vitro and in vivo and is an effective inhibitor of angiogenesis. These findings support the approach of targeting multiple pathways in the search for potential agents with improved anticancer properties.

Keywords Angiogenesis inhibitor · Benzodiazepine · Multikinase inhibitor · Pharmacokinetics · R1530 · Xenografts

Electronic supplementary material The online version of this article (doi:10.1007/s00280-011-1608-x) contains supplementary material, which is available to authorized users.

K. Kolinsky · C. Tovar · H. Yang · D. Carvajal · T. Nevins · K. Packman · B. Higgins (✉)
Discovery Oncology, Hoffmann-La Roche Inc., Nutley, NJ 07110, USA
e-mail: brian_x.higgins@roche.com

Y.-E. Zhang · A. Railkar
Pharmaceutical and Analytical R&D, Hoffmann-La Roche Inc., Nutley, NJ 07110, USA

W. Geng · M. Linn
Department of Non-Clinical Drug Safety, Hoffmann-La Roche Inc., Nutley, NJ 07110, USA

J.-J. Liu · Z. Zhang · P. Wovkulich
Discovery Chemistry, Hoffmann-La Roche Inc., Nutley, NJ 07110, USA

G. Ju
RNA Therapeutics Hoffmann-La Roche Inc., Nutley, NJ 07110, USA

Introduction

Cancers typically rely on a combination of several growth-supportive pathways [1]. Simultaneous targeting of multiple growth pathways can disrupt cellular function, thereby helping to prevent reciprocal growth mechanisms from counteracting a therapeutic benefit and hindering development of chemoresistance [2]. Angiogenesis, the growth

of new blood vessels that involves the endothelial cells adjacent to the tumor, is also pivotal to tumor development [3] and is likewise controlled by multiple pathways [1, 4]. Targeting these pathways simultaneously can render a more thorough ablation of tumors than single-pathway targeting [5–7].

A candidate drug compound that can inhibit diverse cellular mechanisms involved in both tumor cell growth and angiogenesis may potentially have enhanced anticancer activity. In this report, we describe the pharmacokinetic, antitumor, and anti-angiogenic characterization of 5-(2-chlorophenyl)-7-fluoro-1,2-dihydro-8-methoxy-3-methyl pyrazol[3,4-b] [1, 4] benzodiazepine, also known as R1530. This molecule inhibits a number of biochemical targets and thus can modulate multiple pathways identified as being integral to the cell cycle and angiogenesis.

R1530 is a member of a series of benzodiazepine compounds [8] identified as mitotic inhibitors by cell-based screening. We recently reported [9] the screening of R1530 against 178 isolated human kinases using the KINOMEscan platform [10, 11]. R1530 was found to bind to 31 kinases with $K_d < 500$ nM [9]. These 31 kinases included the known cell cycle regulators PLK4 [12–14] and Aurora A [15, 16], as well as the prominent angiogenic kinases VEGFR1, 2 and 3, PDGFRβ, Flt-3, and FGFR1 and 2. In several cancer cell lines in vitro, tubulin polymerization and mitotic checkpoint function were inhibited by exposure to R1530. This disruption led to a predominantly polyploid (>8N) cell population, accompanied by apoptosis or senescence in vitro, and tumor growth inhibition in vivo. Normal (non-cancerous) cells were less sensitive to R1530 [9].

Here, we describe the in vitro antiproliferative activity of R1530 in a number of human tumor and non-transformed cell lines. We further characterize the in vivo antitumor activity of R1530 in a variety of human xenograft models with a range of dosing regimens. The pharmacokinetics of R1530 following single and multiple doses are discussed. Finally, the ability of R1530 to block angiogenesis in vivo is demonstrated using the corneal pocket assay [17].

Materials and methods

Test compound

R1530 was prepared at Hoffmann-La Roche, Inc. The details of the synthetic process will be described in a separate report.

Cell lines and culture

H460, HCT116, HT-29, LoVo, DU145, PC3, SJSA-1, Caki-1, A549, MiaPaCa-2, and NIH-3T3 cells were obtained from American Tissue Culture Collection (Manassas, VA). Lox IMVI cells were obtained from Biological Testing Branch, National Cancer Institute (NCI) (Bethesda, MD). HUVEC cells were obtained from Clonetics (San Diego, CA). The following cell lines were kindly provided by the indicated sources: MDA-MB-435 (P Steeg, NCI, with permission from J Price, University of Texas MD Anderson Cancer Centre [MDACC]); 22rv1 (JW Jacobberger, Case Western University, Cleveland, OH); KB-3-1 (MM Gottesman, NCI); MHM (Norwegian Radium Hospital, Oslo, Norway).

The cell lines were maintained in the following media: MDA-MB-435, PC3, H460, 22rv1, Lox IMVI, A549, DU145, SJSA-1, Caki-1, MHM: RPMI 1640 supplemented with 10% (15% for Caki-1) heat-inactivated fetal bovine serum (HI-FBS) (Gibco/BRL, Gaithersburg, MD); KB-3-1, MIA PaCa-2, NIH-3T3: Dulbecco's Modified Medium with 10% HI-FBS; HCT116, HT-29: McCoys 5A plus 10% HI-FBS; LoVo: F12K plus 10% HI-FBS; HUVEC: EGM-2 (Clonetics).

Cell proliferation assays

Dye exclusion assays

Proliferation was evaluated by the tetrazolium dye assay [18]. Cell lines were plated in a 96-well tissue culture plate (Costar 3595, Corning Inc., Corning, NY) in appropriate medium (180 µl per well) with a seeding density providing logarithmic growth over the course of the assay (5 days). Plates were incubated overnight at 37°C in a humidified environment with 5% CO_2. R1530 was serially diluted 1:3 in corresponding medium resulting in a concentration of 3% DMSO. One-tenth of final volume (20 µl) was then transferred from drug dilution plate to duplicate wells containing cells to give a range of test concentrations starting at 30 µM. The same volume of 3% DMSO in medium was added to a row of control wells. The final concentration of DMSO in all wells was 0.3%. Following incubation for set times (determined by the cells' growth curves), 3-(4,5-dimethylthiazole-2-yl)-2,5-diphenyl-2H-tetrazolium bromide (thiazolyl blue, MTT, Sigma, St. Louis, MO) was added to each well to yield a final concentration of 1 mg/ml. After 2.5-h incubation, the MTT-containing medium was removed and the remaining formazan metabolite was solubilized in 100% ethanol with shaking for 15 min at room temperature. Absorbances were read with a Spectramax Plus Microplate Spectrophotometer (Molecular Devices, Sunnyvale, CA) at 570 nm (650 nm reference).

Inhibition of endothelial cell and fibroblast proliferation

HUVEC were seeded at 10,000 cells per well in 200 µl EGM-2 medium in 96-well flat bottom plates (Costar 3595,

Corning Inc., Corning, NY). After incubation for 24 h at 37°C with 5% CO_2, the incubation medium was aspirated and each well was washed with 300 µl prewarmed EBM-2 containing 50 µg/ml gentamycin and 50 ng/ml amphotercin-B (Clonetics). The washing media was aspirated and replaced with 160 µl per well of serum-starvation medium (EBM-2 supplemented with 1% HI-FBS, [Clonetics]), 50 µg/ml gentamycin and 50 ng/ml amphotercin-B, 10 units/ml heparin (Wyeth-Ayerst, Philadelphia, PA), and 2 mM L-glutamine (Gibco). After 24-h incubation, 20 µl of R1530 stock solutions in serum-starvation medium with 2.5% DMSO was added to the appropriate wells. The control wells contained 20 µl serum-starvation medium with 2.5% DMSO. After preincubating the cells with R1530 for 2 h, 20 µl of growth factor stock solutions in serum-starvation media, basic fibroblast growth factor (bFGF) ([R&D systems 233-FB] 50 ng/ml) or vascular endothelial growth factor (VEGF) ([R&D systems 293-VE] 200 ng/ml) were added. The final concentration of bFGF was 5 ng/ml, and the final concentration of VEGF was 20 ng/ml. The growth factor-free control wells had 20 µl per well of serum-starvation media with 0.01% of bovine serum albumin (BSA) so the final amount of BSA in all the wells were the same. The plates were incubated for an additional 22 h at 37°C with 5% CO_2.

NIH-3T3 fibroblasts were grown in Dulbecco's Modified Eagle Medium (DMEM) (GIBCO/BRL) supplemented with 10% fetal bovine serum (GIBCO/BRL) at 37°C with 5% CO_2. Cells were seeded at 10,000 cells per well in 200 µl of growth medium overnight in 96-well flat bottom plates (Costar 3595, Corning Inc., Corning, NY). Cells were serum starved for 24 h in 160 µl of DMEM (GIBCO/BRL) serum-free medium. R1530 was diluted at 10 times final concentrations in serum starving medium with 1% DMSO, and 20 µl was added in duplicate wells. Control wells had 20 µl of serum starving medium with 1% DMSO. Quiescent cells were preincubated with R1530 at various concentrations for 2 h before the addition of 20 µl of PDGF (R&D systems) at 250 ng/ml to make the final concentration 25 ng/ml. After 24-h exposure to R1530 and PDGF, cells were labeled with WST-1 (Roche Applied Science), a cell proliferation reagent measuring the metabolic activity of viable cells. Cells were incubated with WST-1 for 1 h according to the protocol provided by the company; the formazan formed was quantified at 450 nM with an ELISA plate reader (Molecular Devices, Menlo Park, CA).

Calculation of inhibition

For all assays, the percentage of cell-growth inhibition was calculated using the formula:

$$\text{Percent inhibition} = 1 - [(\text{mean absorbance of experimental wells})/(\text{mean absorbance of control wells})] \times 100.$$

The concentration of R1530 resulting in 50% inhibition of cell proliferation (IC_{50}) was determined from the linear regression of a plot of the logarithm of the concentration versus percent inhibition. The IC_{50} values were determined by Excel fit sigmoidal dose–response model.

Animals

Female athymic Crl:NU-Foxn1^{nu} nude mice were used for efficacy testing, and female C57BL/6 mice were used for corneal neoangiogenesis assays (Charles River, Wilmington, USA). Mice were 10–12 weeks of age and weighed 23–25 g at the time of study initiation. The health of the mice was assessed daily by observation, and blood samples for analysis were taken from sentinel animals on shared shelf racks. All animals were allowed to acclimate for 1 week. Autoclaved water and irradiated food (5058-ms Pico Lab mouse chow, Purina Mills, Richmond, IN) were provided ad libitum. The animals were kept in a 12-h light and dark cycle. Cages, bedding, and water bottles were autoclaved before use and changed weekly. All animal experiments were conducted in accordance with the Guide for the Care and Use of Laboratory Animals, local regulations, and protocols approved by the Roche Animal Care and Use Committee in an AAALAC accredited facility.

Single-dose pharmacokinetic analysis

R1530 was formulated in PEG400 and hydroxypropyl beta cyclodextrin 28% w/w with 0.1% Tween 80 for the intravenous (iv) dosing, and a 1% Klucel LF in water with 0.1% Tween 80 suspension for the oral (po) administration. The iv dose was 5 mg/kg and the po doses were 25, 100, 200, 300 mg/kg.

Blood samples were collected from three independent nude mice at each timepoint under anesthesia from the retro-orbital sinus or via terminal cardiac puncture into tubes containing EDTA as anticoagulant. Samples were collected at 5, 15, and 30 min and 1, 2, 4, 8, 16, and 24 h after a single iv dose and at 15 and 30 min, and 1, 2, 4, 8, 16 and 24 h after a single po dose of R1530.

Plasma was stored at −70°C until analysis. The plasma samples were analyzed by LC–MS/MS. The calibration curves ranged from 50 to 5,000 ng/ml. Parameters were estimated by applying noncompartmental pharmacokinetics to the plasma concentration versus time data. Standard and QC samples were injected together with study samples. All concentrations were interpolated from calibration

curves ranging from 1 to 2,000 ng/ml using an internally validated Watson laboratory information system (LIMS) software program (version 6.3.0.01a).

Mouse xenograft studies and end of study pharmacokinetic analysis

All cell lines were cultured and scaled up using standard in vitro methods using the reagents as described above. For subcutaneous tumor inoculations into the right flank (or inguinal fat pat for MDA-MB-435), each mouse received 3×10^6 (HCT116), 5×10^6 (LoVo), 7.5×10^6 (A549), 1×10^7 cells (H460, MDA-MB-435, 22rv1) in 0.2 ml phosphate-buffered saline (PBS) or 1:1 PBS + phenol-free Matrigel (BD Biosciences, Franklin Lakes, NJ) (MDA-MB-435, 22rv1). Typically, when palpable tumors were established, animals were randomized so that all groups had 10 mice with no statistically significant differences in starting mean tumor volumes ($P < 0.05$, range 100–150 mm^3).

R1530 was formulated as a suspension in 1% Klucel LF in water with 0.1% Tween for po administration at a constant volume based on average mouse body weight (0.2 ml per injection). Formulated compound was made up weekly, stored at 4°C in amber vials and vortexed immediately prior to administration. Details of the frequency and number of doses are specified in the Results section.

In situ tumor measurements and mouse body weights were recorded two to three times per week. Animals were individually monitored throughout the experiment. Toxicity was assessed by measuring changes in body weight and gross observation of individual animals.

To determine the plasma levels of R1530, blood samples were collected, stored, and processed, in the same way as described for the single-dose pharmacokinetic experiments except sets of three of the same mice that were serially bled twice for 1 and 8 h timepoint and 4 and 24 h timepoints, respectively. Samples were collected at 1, 4, 8, and 24 h following the final dose.

Calculations and statistical analysis

Weight loss was calculated as percent change in mean group body weight, using the formula:

$$((W - W_0)/W_0) \times 100$$

where 'W' represents mean body weight of the treated group at a particular day, and 'W_0' represents mean body weight of the same group at start of treatment. Maximum weight loss was also calculated using the formula above, giving the maximum percentage of body weight lost at any time in the entire experiment for a particular group. Toxicity was defined as mortality and/or ≥20% individual body weight loss in 20% of the mice.

Treatment efficacy was assessed by tumor growth inhibition (TGI). Tumor volumes of treated groups were calculated as percentages of tumor volumes of the control groups (%T/C), using the formula:

$$100 \times ((T - T_0)/(C - C_0))$$

where 'T' represents mean tumor volume of a treated group on a specific day during the experiment, 'T_0' represents mean tumor volume of the same group on the first day of treatment, C represents mean tumor volume of a control group on a particular day of the experiment, and C_0 represents mean tumor volume of the same group on the first day of treatment. TGI was calculated using the formula:

$$100 - (\%T/C).$$

As defined by NCI criteria, ≥60% TGI is considered biologically significant (Johnson et al. [14]).

Tumor volume (mm^3) was calculated using the ellipsoid formula:

$$(D \times (d^2))/2$$

where 'D' represents the large diameter of the tumor, and 'd' represents the small diameter.

Statistical analysis was by the Mann–Whitney rank sum test (SigmaStat, version 2.03). The significance level was set at $P \leq 0.05$.

For the survival assessment, animals were evaluated for tumor re-growth following cessation of treatment. The percentage survival was plotted against time from tumor implant. Tumor re-growth to a historically predefined tumor line–specific volume (LoVo: 400 mm^3; A549, MDA-MB-435: 500 mm^3; H460, HCT116: 1,000 mm^3; 22rv1: 1,500 mm^3) was considered as a surrogate for death when calculating increased life span (ILS). ILS was calculated as: $100 \times$ [(median survival day of treated group −median survival day of control group)/median survival day of control group] Median survival was determined utilizing the Kaplan–Meier survival analysis (Stat View, SAS). More than 25% ILS is biologically significant, as defined by NCI criteria [19].

In vivo inhibition of angiogenesis

The effects of R1530 on corneal neoangiogenesis were assessed in the corneal pocket assay (CPA) in 8 female C57BL/6 mice per group in both bFGF- and VEGF-driven assays. A pellet impregnated with growth factor (90 ng bFGF or 180 ng VEGF) was implanted in the base of a pocket made in the cornea, to stimulate vessel growth from the limbus toward the pellet, as described previously [17]. R1530 treatment (50 mg/kg qd po) was initiated on the same day as implantation. In the bFGF assay, animals were

dosed for 5 days while in the VEGF assay animals were dosed for 7 days prior to quantitation of the area of vascularization using slit lamp microscopy. The circumferential zone of neovascularization was measured as clock hours. The vessel length and clock hour of corneas from treated animals was compared to that of vehicle-treated animals to determine the extent of inhibition.

On the last day of treatment in the VEGF CPA (day 7), the femur and tibia were collected from the mice for assessment of epiphyseal growth plate thickness. Hind limbs were formalin fixed and tissues were trimmed, processed, embedded in paraffin, sectioned, mounted on glass microscope slides, and stained with hematoxylin and eosin (H&E).

Results

Inhibition of cell proliferation by R1530

The potent in vitro antiproliferative activity of R1530 in a range of human tumor cell lines is demonstrated by the IC_{50} values shown in Table 1. All cell lines evaluated were sensitive to R1530, regardless of the tissue of origin; IC_{50} values ranged from 0.22 to 3.43 μM. The most potent inhibition was observed in the MDA-MB-435 breast tumor cells.

The antiproliferative activity of R1530 was further characterized by its effects on VEGF- and bFGF-induced proliferation of human endothelial cells and PDGF-driven fibroblast proliferation. R1530 strongly inhibited HUVEC growth driven by either VEGF or bFGF (Table 1). The IC_{50} for VEGF-driven HUVEC growth (49 nM) was lower than that for bFGF-induced growth (118 nM). R1530 was less active in the PDGF-driven assay with an IC_{50} of 688 nM.

Table 1 Inhibition of cell growth by R1530

Histotype	Cell line	IC_{50} (μM)
Breast	MDA-MB-435	0.22
Colon	HCT116	0.68 ± 0.20*
	HT-29	1.00 ± 0.30**
Lung	H460	0.73 ± 0.22*
Prostate	DU145	2.03
	22rv1	0.84
	PC3	1.65
Bone	SJSA-1	0.95
	MHM	1.52
Pancreas	MIA PaCa-2	3.43
Renal	Caki-1	1.60 ± 0.10***
Melanoma	Lox IMVI	0.70
Epidermoid (oral)	KB-3-1	0.50
Endothelial	VEGF-driven HUVEC	0.049 ± 0.025***
	FGF-driven HUVEC	0.118 ± 0.081***
Fibroblast	PDGF-driven NIH-3T3	0.688 ± 0.305[§]

All assays were performed once in triplicate wells, except the following: * $n = 6$, ** $n = 2$, *** $n = 4$, [§] $n = 3$. Note these values show standard deviations

Single-dose pharmacokinetics of R1530

Results of pharmacokinetic analyses following a single dose of R1530 are shown in Table 2. After a single iv dose of R1530 (5 mg/kg), a moderate total plasma clearance of 8.8 ml/min/kg was observed with an extensive tissue distribution ($V_{ss} = 3.12$ l/kg) and an elimination half-life of 4.32 h. The mean maximum plasma concentration of R1530 was reached 2 h after an oral dose of 25 or 100 mg/kg, and 4 h after an oral dose of 200 or 300 mg/kg. Although 100% bioavailability (complete absorption) of R1530 was observed from oral doses of 25 and 100 mg/kg in nude mice, bioavailability was reduced to 67 and 40% for 200 and 300 mg/kg, respectively, and exposure did not increase compared to 100 mg/kg. Therefore, subsequent efficacy testing of doses greater than 100 mg/kg was not conducted.

Efficacy of once-daily oral dosing of R1530 in H460 non-small-cell lung cancer (NSCLC) xenografts

The tolerability and in vivo antitumor activity of R1530 qd for 19 days po was assessed in nude mice bearing human H460 NSCLC xenografts. Toxicity grossly manifested as >20% body weight loss (i.e. morbidity), and mortality was evident by day 5 in mice receiving 100 mg/kg qd R1530, and this group was terminated. No signs of toxicity or significant body weight loss were noted in mice dosed with 0.78, 1.56, 3.125, 6.25, 12.5, 25, and 50 mg/kg qd R1530 (data not shown). Therefore, 50 mg/kg was the maximum tolerated dose (MTD) of R1530 qd.

Figure 1 illustrates the effect of once-daily R1530 on tumor growth in the H460 human NSCLC xenograft model. The lowest dose at which significant antitumor activity was observed was 3.125 mg/kg qd (72% TGI, $P < 0.001$). At 6.25 and 12.5 mg/kg, TGIs of 83% ($P < 0.001$) and 92% ($P < 0.001$), respectively, were seen. At the higher doses of 25 and 50 mg/kg qd, 96% TGI ($P < 0.001$, with 2/9 partial responses [PRs]) and >100% TGI ($P < 0.001$, 9/10 PRs and 1/10 complete regressions [CRs]) were observed, respectively (Fig. 1a). Tumors exposed to R1530 were smaller and paler in appearance than tumors from mice treated with

Table 2 R1530 pharmacokinetic parameters following a single intravenous dose (5 mg/kg) or a single oral dose (25, 100, 200 or 300 mg/kg)

Parameter	Mean overall value				
	5 mg/kg intravenous	25 mg/kg oral	100 mg/kg oral	200 mg/kg oral	300 mg/kg oral
T_{max} (h)	0.08333	2	2	4	4
C_{max} (ng/ml)	2,270	5,070	20,100	22,100	19,100
AUC (ng·h/ml)	9,470	46,700	225,000	254,000	266,000
AUC/dose (ng·h/ml/mg/kg)	1,890	1,870	2,250	1,270	760
Bioavailability, F (%)		100	100	67	40
MRT (h)	6.01				
V_{dss} (ml/kg)	3,120				
$T_{1/2}$ (h)	4.32				
$CL_{(0-t)}$ (ml/kg/h)	528				
AUC extrapolated (ng·h/ml)	9,640				
AUC extrapolated/dose (ng·h/ml/mg/kg)	1,930				
% AUC extrapolated	1.73				

vehicle (see supplementary information). This observation is consistent with the anti-angiogenic activity attributed to R1530.

The vehicle-treated group was terminated on day 29 postimplantation due to tumor burden. However, mice in the R1530-treated groups were monitored until individual tumor volumes reached 1,000 mm^3, a surrogate endpoint for 'survival'. The Kaplan–Meier cumulative survival plot for each dose group is shown in Fig. 1b. There was a biologically significant increase in survival (≥25%) in all dose groups with the maximum increased life span (ILS) reached being 132% for the 50 mg/kg qd group ($P < 0.0001$ vs vehicle control).

Plasma exposure levels of R1530 from biologically active groups from this study are shown in Fig. 1c. No evidence of accumulation was observed after repeated administration of 25 mg/kg qd in nude mice compared to single administration (Table 2). The total plasma exposure level (C_{max}) increased with increasing dose in a slightly greater than dose proportional manner.

A confirmatory study in the same xenograft model with dosing at 6.25, 12.5, 25, and 50 mg/kg qd for 14 days was

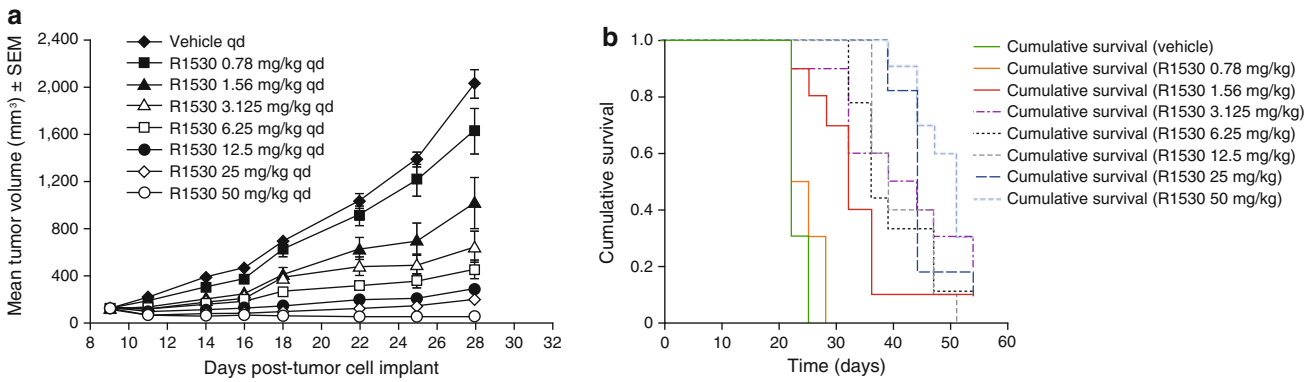

c

Original dose (mg/kg, qd)	T_{max} (hours)	C_{max} (ng/mL)	AUC (ng• hours/mL)	AUC/dose (ng• hours/mL/mg/kg)
1.56	1	285	3,040	1,950
3.125	1	786	7,680	2,460
6.25	1	1,780	15,700	2,510
12.5	1	4,910	43,600	3,480
25	1	7,300	56,200	2,250
50	1	9,020	112,000	2,230

Fig. 1 **a** Antitumor activity of R1530 (0.78–50 mg/kg qd) in H460 human non-small-cell lung cancer (NSCLC) xenografts in nude mice. Values are means ± SEM ($n = 10$/group); **b** Kaplan–Meier survival analysis of nude mice bearing H460 human NSCLC xenografts treated with R1530; **c** pharmacokinetic parameters of R1530 measured on the final day of dosing

performed. Again, significant tumor growth inhibition ($P < 0.001$) was observed at all doses (data not shown, see supplementary information).

Efficacy of once- and twice-weekly oral R1530 in nude mice bearing H460 NSCLC xenografts

In the same xenograft model, no signs of toxicity were noted in mice receiving R1530 in qw doses of 25, 50 and 100 mg/kg, or a biw dose of 100 mg/kg for approximately 3 weeks (data not shown).

Figure 2 shows the effect of these dosing schedules on tumor growth. Statistically significant TGI was observed only in mice treated with the highest dose (100 mg/kg qw), resulting in 66% TGI ($P < 0.001$). The doses of 25 and 50 mg/kg gave 27 and 57% TGI, respectively, which were not significant. At 100 mg/kg biw, 80% TGI was observed ($P < 0.001$). Based on these results compared with those described above, once-daily dosing appeared to be significantly more efficacious than less frequent dosing. Thus, daily oral dosing was selected for further evaluation in other tumor models.

Anti-tumor activity of R1530 in other human xenograft models

To assess the broader activity of R1530, a range of human tumor xenograft models were tested for sensitivity to doses of either 25 and 50 mg/kg qd or 1.56 and 50 mg/kg qd for approximately 3 weeks. Data from these experiments are summarized in Table 3, showing the effect this treatment had on tumor growth and survival.

In the A549 NSCLC model, 50 mg/kg qd had potent antitumor and survival effects with >100% TGI ($P < 0.001$), 3/9 PRs, 6/9 CRs, and an ILS of 118% ($P = 0.0002$). Antitumor activity and survival effects were not biologically meaningful in animals treated with 1.56 mg/kg qd R1530, mirroring what was seen in the H460 model at that dose.

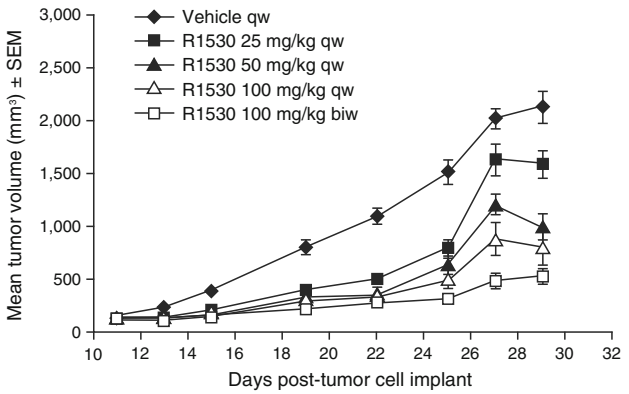

Fig. 2 Antitumor activity of R1530 (25 mg/kg qw–100 mg/kg biw) in H460 human NSCLC xenografts in nude mice. Values are means ± SEM ($n = 10$/group)

In a breast ductal adenocarcinoma model (MDA-MB-435), R1530 induced >100% TGI with both 25 and 50 mg/kg qd treatment (both $P < 0.001$), with 7/9 and 10/10 PRs, respectively. The greatest increase in survival was observed in this model, where 163 and 233% ILS (both $P < 0.0001$) were observed in the 25 and 50 mg/kg treated groups, respectively.

Greater than 100% TGI was observed in the 22rv1 andogen-independent prostate carcinoma model with 50 mg/kg qd R1530. All 10 mice experienced a PR ($P < 0.001$), and the ILS was 133% ($P < 0.0001$) in this group. In mice receiving 25 mg/kg qd R1530, the TGI was 98%, with 4/10 PRs observed and an ILS of 67% ($P < 0.0001$).

In the LoVo colorectal adenocarcinoma model, both 25 and 50 mg/kg qd R1530 dose groups showed >100% TGI (both $P < 0.001$), and 66% ILS (both $P < 0.0001$) compared with vehicle control. Five and nine out of 10 mice achieved PRs in the 25 and 50 mg/kg qd groups, respectively.

Tumor growth was inhibited by >100% ($P < 0.001$) in the colorectal carcinoma model HCT116 with 50 mg/kg qd R1530. All 10 mice achieved PRs and a corresponding 62% ILS ($P < 0.0001$) was seen in this group. Antitumor activity and survival effects were not biologically meaningful in animals treated with 1.56 mg/kg qd R1530, similar to the H460 and A549 models.

Inhibition of VEGF and bFGF experimentally induced angiogenesis in the murine cornea and induction of physeal hyperplasia by daily oral R1530 administration

The effect of R1530 on corneal neoangiogenesis was assessed in the corneal pocket assay (CPA) with administration of 50 mg/kg qd R1530 po commencing on the day of surgical implantation of bFGF- or VEGF-impregnated pellets. Complete blockade of angiogenesis was observed in both the bFGF CPA and the VEGF CPA (Fig. 3a). Angiogenesis was inhibited 99% compared to vehicle-treated animals ($P = 0.021$, $P \leq 0.001$, respectively).

After dosing was complete, the femur and tibia were collected from the mice for the assessment of epiphyseal growth plate thickness. Consistent with findings from the CPA, minimal-to-mild hypertrophy of the femoral growth plate (Fig. 3b) and the tibial growth plate (not shown) was observed in all six mice treated with R1530. The tibial growth plate in rodents is affected by angiogenic processes [22]; similar changes in growth plates are associated with treatment by anti-angiogenic agents [23].

Table 3 Summary of antitumor activity of qd R1530 in nude mice in a range of human xenograft models

Cell Line	Dose (mg/kg)	% TGI*	*P* value (vs. vehicle)	Partial regressions	Complete regressions	% ILS*	*P* value (vs. vehicle)
A549	1.56	11	0.034	0/10	0/10	6	0.4127
	50	>100	<0.001	3/9	6/9	118	0.0002
MDA-MB-435	25	>100	<0.001	7/9	0/9	163	<0.0001
	50	>100	<0.001	9/10	0/10	233	<0.0001
22rv1	25	98	<0.001	4/10	0/10	67	<0.0001
	50	>100	<0.001	10/10	0/10	133	<0.0001
LoVo	25	>100	<0.001	5/10	0/10	66	<0.0001
	50	>100	<0.001	9/10	0/10	66	<0.0001
HCT116	1.56	38	0.717	0/10	0/10	7	<0.0001
	50	>100	<0.001	10/10	0/10	62	<0.0001

* As defined by NCI criteria, TGI ≥60% and ILS ≥25% are biologically significant [19]

Discussion

R1530 is a pyrazolobenzodiazepine, which has been shown to inhibit kinases that regulate multiple pathways involved in tumor cell cycle regulation and angiogenesis. The ability of a compound to inhibit an array of tumorigenic mechanisms is a desirable characteristic for potentially wide-ranging therapeutic activity and to minimize development of resistance to chemotherapeutic agents. Here, we have shown that R1530 inhibits proliferation of multiple tumor cell lines in vitro and has antitumor and anti-angiogenic activity in vivo.

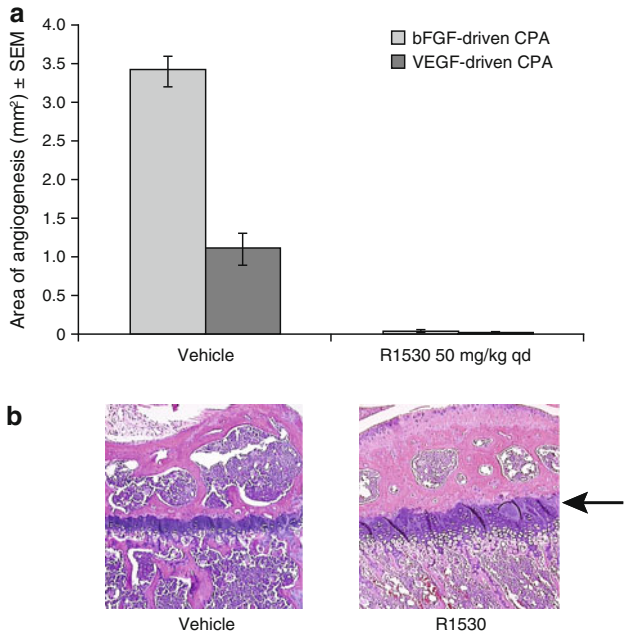

Fig. 3 **a** Effect of R1530 on corneal angiogenesis in C57/B16 mice, driven by bFGF and VEGF. **b** Representative H&E section of femur epiphyseal growth plate. *Arrow* indicates minimal-to-mild hypertrophy of the femoral growth plate

In a previous study [9], we hypothesized that inhibition of several kinases, which regulate cell division, had a potential role in the mechanism of action of R1530 in inducing polyploidy and disrupting proliferation of tumor cells in vitro. In this work, we have expanded the investigation into in vitro antiproliferative activity of R1530 to include a broad spectrum of human tumor cell lines. Micromolar IC_{50} values of R1530 in all cell lines studied demonstrated the potent activity of R1530 regardless of the tissue of origin. In addition, R1530 also strongly inhibited the proliferation of endothelial cells driven by VEGF and FGF in vitro, with IC_{50} values of below 0.05 μM in the VEGF-driven assay. Moderate activity of R1530 against PDGF-driven fibroblast proliferation was also described. The potency of R1530 in these angiogenic growth factor-driven cell proliferation assays correlates well with the previously reported inhibition by R1530 of the angiogenic kinase activities of VEGFR-2, FGFR, and PDGFR-β [9].

The in vitro antiproliferative properties of R1530 were correlated with the significant antitumor activity observed in vivo. We have previously reported that twice-daily doses of 25 mg/kg R1530 in mice bearing H460 NSCLC human NSCLC xenografts resulted in >100% tumor growth inhibition, and PRs in 10/10 animals [9]. We report herein that R1530 dosed once daily also had marked antitumor activity with significant tumor regression (96% TGI) at the MTD of 50 mg/kg qd. Efficacy was also demonstrated with once- and twice-weekly dosing of R1530, but the effects of these regimens on tumor growth were not as pronounced as the daily doses. More frequent dosing is therefore favored for optimal R1530 antitumor activity.

In another NSCLC model (A549), R1530 dosed at 50 mg/kg qd resulted in complete tumor remission in two-thirds of the mice after 3 weeks of treatment, with the

remainder experiencing PRs. The TGI in this dose group was >100%. A549 is a slow-growing tumor so is expected to rely more on angiogenesis than the faster-growing H460 [20, 21]. The increased activity of R1530 against A549 compared with H460 supports the hypothesized anti-angiogenic properties of R1530 in vivo.

The antitumor activity of once-daily doses of R1530 demonstrated in NSCLC models was confirmed in other human tumor models, including breast, prostate, and colorectal xenografts. In these studies, once-daily R1530 at the MTD of 50 mg/kg resulted in tumor regression in all tested tumor types. Partial rather than full regressions predominated in all these models. Tumor regression (>100% TGI) was observed in two of the three models where ½ MTD (25 mg/kg qd) R1530 was tested (LoVo colorectal adenocarcinoma, MDA-MB-435 breast ductal adenocarcinoma). In the third model (22rv1 andogen-independent prostate carcinoma), treatment resulted in 98% TGI.

Survival, measured as the time taken for tumors to reach a historically predefined tumor volume posttreatment, was biologically significantly increased in all groups dosed with 25 or 50 mg/kg R1530 compared with vehicle-treated mice, regardless of the xenograft model tested. The largest increase in life span with R1530 treatment was observed in the MDA-MB-435 breast ductal adenocarcinoma model, where 163 and 233% increases were observed in the 25 and 50 mg/kg treated groups, respectively.

Pharmacokinetic data obtained following single oral doses of R1530 in nude mice indicated that the compound had excellent oral bioavailability and PK properties that favor daily dosing. There was a dose-dependent increase in exposure achieved up to a dose of 100 mg/kg and exposure did not increase at 200 or 300 mg/kg. Thus, doses higher than 100 mg/kg were not evaluated in efficacy studies. The pharmacokinetic data also demonstrated no accumulation of R1530 in plasma pharmacokinetic measurements after repeated administration. This observation is in agreement with the exposure data from our previous in vivo experiments (data not shown).

The ability of R1530 to block the activity of VEGFR and FGFR signaling in vivo was assessed using an experimental system, the murine CPA [17]. Corneal angiogenesis stimulated by both bFGF and VEGF was 99% inhibited when R1530, at the once-daily MTD of 50 mg/kg, was administered. VEGF plays an important role during endochondral bone formation in hypertrophic cartilage remodeling [22] and has been shown to be disrupted by compounds that target VEGF [23]. All mice treated in the VEGF CPA showed minimal-to-mild hypertrophy of the femoral and tibial growth plate. This finding was consistent with a systemic blockade of VEGF-driven angiogenesis by R1530.

In summary, we have shown that R1530 inhibits tumor growth by blocking a variety of tumorigenic and angiogenic pathways. Once-daily dosing of R1530 in mice had comparable antitumor activity across a broad range of human xenograft models. At doses which resulted in significant growth inhibition and tumor regression and a significant improvement in survival, there was no observed toxicity. These data indicate that R1530 may have antitumor activity in a clinical setting. Future preclinical studies will explore the antitumor activity of R1530 in combination with commonly used chemotherapeutic agents. R1530 has progressed to clinical testing.

Acknowledgments The authors would like to thank Enrique Calderon, David Malcolm, Vanderlei Goncalves from the Roche Comparative Medicine group for their technical support. Fei Su and David Heimbrook for critical review of the manuscript and Steve Middleton for his project management. Medical writing support was provided by Tom Westgate of Gardiner-Caldwell Communications, funded by Roche. All authors are remunerated employees of Hoffman-La Roche, Inc.

References

1. Hanahan D, Weinberg RA (2000) The hallmarks of cancer. Cell 100:57–70
2. Odoux C, Albers A (2004) Additive effects of TRAIL and paclitaxel on cancer cells: implications for advances in cancer therapy. Vitam Horm 67:385–407
3. Folkman J (1992) The role of angiogenesis in tumor growth. Semin Cancer Biol 3:65–71
4. Folkman J (1997) Tumor angiogenesis. In: Holland JF, Bast RC, Morton DL, Frei E, Kufe DW, Weichselbaum RR (eds) Cancer medicine. Williams and Wilkins, Baltimore, MD, pp 181–204
5. Folkman J (1972) Anti-angiogenesis: new concept for therapy of solid tumors. Ann Surg 175:409–416
6. Folkman J (2007) Angiogenesis: an organizing principle for drug discovery? Nat Rev Drug Discov 6:273–286
7. Ruegg C, Mutter N (2007) Anti-angiogenic therapies in cancer: achievements and open questions. Bull Cancer 94:753–762
8. Sternbach LH (1978) The benzodiazepine story. Prog Drug Res 22:229–266
9. Tovar C, Higgins B, Deo D, Kolinsky K, Liu J-J, Heimbrook DC, Vassilev LT (2010) Small-molecule inducer of cancer cell polyploidy promotes apoptosis or senescence: implications for therapy. Cell Cycle 9:3364–3375
10. Goldstein DM, Gray NS, Zarrinkar PP (2008) High-throughput kinase profiling as a platform for drug discovery. Nat Rev Drug Discov 7:391–397
11. Fabian MA, Biggs WH III, Treiber DK, Atteridge CE, Azimioara MD, Benedetti MG, Carter TA, Ciceri P, Edeen PT, Floyd M, Ford JM, Galvin M, Gerlach JL, Grotzfeld RM, Herrgard S, Insko DE, Insko MA, Lai AG, Lelias JM, Mehta SA, Milanov ZV, Velasco AM, Wodicka LM, Patel HK, Zarrinkar PP, Lockhart DJ (2005) A small molecule-kinase interaction map for clinical kinase inhibitors. Nat Biotechnol 23:329–336
12. Li JJ, Li SA (2006) Mitotic kinases: the key to duplication, segregation, and cytokinesis errors, chromosomal instability, and oncogenesis. Pharmacol Ther 111:974–984

13. Habedanck R, Stierhof YD, Wilkinson CJ, Nigg EA (2005) The Polo kinase Plk4 functions in centriole duplication. Nat Cell Biol 7:1140–1146
14. Johnson EF, Stewart KD, Woods KW, Giranda VL, Luo Y (2007) Pharmacological and functional comparison of the polo-like kinase family: insight into inhibitor and substrate specificity. Biochemistry 46:9551–9563
15. Vader G, Lens SM (2008) The Aurora kinase family in cell division and cancer. Biochim Biophys Acta 1786:60–72
16. Barr AR, Gergely F (2007) Aurora-A: the maker and breaker of spindle poles. J Cell Sci 120:2987–2996
17. Kenyon BM, Voest EE, Chen CC, Flynn E, Folkman J, D'Amato RJ (1996) A model of angiogenesis in the mouse cornea. Investig Opthalmol Vis Sci 37:1625–1632
18. Denizot F, Lang R (1986) Rapid colorimetric assay for cell growth and survival. Modifications to the tetrazolium dye procedure giving improved sensitivity and reliability. J Immunol Methods 89:271–277
19. Johnson JI, Decker S, Zaharevitz D, Rubinstein LV, Venditti JM, Schepartz S, Kalyandrug S, Christian M, Arbuck S, Hollingshead M, Sausville EA (2001) Relationships between drug activity in NCI preclinical in vitro and in vivo models and early clinical trials. Br J Cancer 84:1424–1431
20. Kerbel R, Folkman J (2002) Clinical translation of angiogenesis inhibitors. Nat Rev Cancer 2:727–739
21. Higgins B, Kolinsky K, Smith M, Beck G, Rashed M, Adames V, Linn M, Wheeldon E, Gand L, Birnboeck H, Hoffmann G (2004) Antitumor activity of erlotinib (OSI-774, Tarceva) alone or in combination in human non-small cell lung cancer tumor xenograft models. Anticancer Drugs 15:503–512
22. Petersen W, Tsokos M, Pufe T (2002) Expression of VEGF121 and VEGF165 in hypertrophic chondrocytes of the human growth plate and epiphyseal cartilage. J Anat 201:153–157
23. Hall AP, Westwood FR, Wadsworth PF (2006) Review of the effects of anti-angiogenic compounds on the epiphyseal growth plate. Toxicol Pathol 34:131–147